PhD in Molecular and Experimental Medicine - XXXV cycle

The novel lncRNA *Chheaf-1* regulates cardiac hypertrophy via *Rtn4*

Candidate:

Javier Laura Francés

ID Number:

4K001755

Thesis Supervisor

Prof. Gianluigi Condorelli

Co-Supervisor

Dr. Christina Pagiatakis

Academic Year 2021 – 2022

TABLE OF CONTENTS

ABSTRACT

Cardiovascular diseases are the leading cause of mortality and morbidity worldwide. One of the more prevalent conditions is cardiac hypertrophy, which develops into heart failure. The non-coding transcriptome plays a central role in the regulation of cardiomyocyte hypertrophy, but has yet to be exploited for novel therapies. Thus, we screened cardiomyocyte-enriched long-noncoding RNAs in a model of pressure overload in mice. Interestingly, we discovered more than 150 dysregulated long non-coding RNAs (lncRNAs), suggesting their importance in the maintenance of cardiac homeostasis. Amongst the dysregulated lncRNAs, we identified a novel non-coding transcript, *Gm12092* which we named "Cardiac hypertrophy and heart failure-1", (*Chheaf-1*) that regulates hypertrophic onset upon pressure overload in mice though its neighboring gene *Rtn4* (Nogo-A), which has been shown to be important for maintaining proper cardiac function. *Chheaf-1* is a nuclear and cardiac-enriched lncRNA that exerts a protective role on the heart after pressure overload. In order to evaluate the role of *Chheaf-1,* we generated a constitutive knockout (KO) mouse model, *Chheaf-1*$^{-/-}$. When subject to transverse aortic constriction (TAC), a murine model of pressure overload, *Chheaf-1*$^{-/-}$ mice present a significant decrease of cardiac function. Previous studies in an inducible cardiomyocyte-specific knockout of Nogo-A have shown than in the absence of Nogo-A during pressure overload, there is an accumulation of ceramides that prevents beneficial autophagy and leads to severe heart failure. Interestingly, *Chheaf-1*$^{-/-}$ mice exhibit insufficient levels of Nogo-A after pressure overload, and an absence of autophagy-related markers. Autophagy markers and cardiac function were restored when treating *Chheaf-1*$^{-/-}$ mice with myriocin, compound that blocks ceramide synthesis. *Chheaf-1* regulates *Rtn4* expression through deposition of H3K27ac, which we hypothesize is a result of the recruitment of the Gata4/p300 complex. Finally, we discovered a human ortholog for *Chheaf-1*, based on synteny and epigenetic landscape, which provides a very promising translational application of this lncRNA.

ACKNOWLEDGEMENTS

Echocardiography and Surgeries: Arianna Felicetta, Pierluigi Carullo, **Bioinformatic analysis**: Simone Serio, **Lab members**: Laura Papa, Roberto Papait. **Collaborators:** Annarita di Lorenzo, Ju Chen **Humanitas genomic facility, Humanitas FACs facility, Supervision:** Christina Pagiatakis and Gianluigi Condorelli.

INTRODUCTION

Cardiovascular diseases (CVD) are the leading cause of death worldwide, and the incidence of CVD continues to increase around the world with changes in lifestyle and increase in the average lifespan. Previous studies reported that only in Europe, around 4 million people die of CVD every year, accounting for 44% of all deaths (1).

The mechanisms underlying cardiac hypertrophy and heart failure have been studied widely over the last several decades, and, although much is known about the pathways involved in disease onset, therapeutic strategies still remain elusive. The etiology of hypertrophy can vary, including genetic defects that lead to hypertrophic cardiomyopathy (HCM). HCM has an incidence of 1:500 and it is predicted to affect 1 million people within the EU. Moreover, ventricular hypertrophy can arise as a consequence of arterial stenosis or arterial hypertension. Pathological cardiac hypertrophy is the heart's response to a wide variety of extrinsic and intrinsic factors that produce a biomechanical stress to the heart, developing into an increase in size of the ventricular chambers to offset the loss of contractile force. At the cellular level, ventricular cardiomyocytes grow in size, increase protein production, re-organize their sarcomere, switch their metabolism, and turn to an embryonic-like gene programming state.

There is growing evidence that these rearrangements in cardiomyocytes are, in part, governed by epigenetic mechanisms. Epigenetics refers to all the changes produced in heritable traits due to modulation of gene expression without affecting the DNA sequence. Some of the epigenetic mechanisms affecting the heart include DNA methylation, post-translational modifications of histones, adenosine triphosphate (ATP)-dependent chromatin conformation and remodeling, and non-coding RNA regulation (2).

DNA methylation was associated with transcriptional repression. More than a decade ago Movassaghetal *et al* (3), demonstrated a decreased methylation in promoters in failing hearts. These promoters were further correlated to well-known pro-hypertrophic genes (4). Furthermore, thanks to the development of 'omics' science, more extensive research showed which specific regions of the genome are subjected to hypo- or hyper-methylation in the onset of hypertrophy in patients (5). Interestingly, we now know that DNA methylation can be associated with both active and repressed transcription, indicating a more diversified role of DNA methylation in regulating gene expression as previously believed. Genes up- or down-regulated by DNA methylation seem to be associated with regulation of different compartments of the cells: upregulated genes are related to nuclear structural genes, while downregulated genes with extracellular features (6).

Moreover, post-translational modifications to histones are also required for the regulation of transcription. Histone proteins are necessary for the wrapping of DNA in order to compact the chromatin and form the nucleosome. Post-translational modifications to histone tails are therefore necessary for promoting a relaxation or a condensation of the chromatin that is linked to a more active or repressed transcription status, respectively. These modifications depend not only on the position of the modification, but also on the nature of the modification (acetylation, methylation, phosphorylation, ubiquitylation, and sumoylation). Histone modifications change chromatin structure influencing DNA accessibility to various regulatory elements including transcription factors. For example, a well-known modification is acetylation of histone H3 at the lysine 27 (K) residue (H3K27Ac), that marks active enhancers and promoter regions, while tri-methylation of the same residue is a repression mark (H3K27me3) (7). Histone residues are modified (among others) by histone acetyltransferases (HATs) and histone deacetylases (HDACs), that affect gene expression patterns in association to transcription factors that are recruited as a result of these modifications (8).

H3K27Ac is mediated, in part, by the histone acetyl transferase (HAT) protein p300, that in the case of the heart, is a well-known co-activator of the transcription factor (TF) Gata4, promoting fetal and hypertrophic gene expression during pressure overload (9). Cardiac-overexpression of p300 in mouse produced an increased DNA binding capacity of Gata4 to its downstream targets, including the known pro-hypertrophic genes *NppA*, *Endothelin*-1 and *B-myosin heavy chain 7* (*Myh7*) (10). Opposite results were observed when the activity of p300 was

chemically blocked (11). Mechanistically, pressure overload stress induces activation of kinases such as Protein Kinase B (Akt) or mitogen-activated protein kinase (Mapk), that lead to the phosphorylation of p300 increasing its HAT activity. p300 mediates the acetylation of TFs such as Mef2 and Gata4 to promote pro-hypertrophic gene re-programming (12). Gata4 is essential for cardiac development and the hypertrophic response, and it collaborates with Mef2a (myocyte enhancer factor 2A), Mef2c (myocyte enhancer factor 2C) and Nkx2-5 (NK2 homeobox 5) to regulate its target genes (12). Gata4 deletion causes embryonic lethality related to endodermal defects and cardiac malformation. Additionally, Gata4 knockout in cardiomyocytes of adult mice compromised their cardiac function against pressure overload, highlighting its anti-hypertrophic potential (13). One of the most studied signaling pathways in response to hypertrophy is the activation of cardiac fetal genes by Gata4/Nfat3 in a calcineurin-dependent manner, in response to intercellular Ca^{2+} accumulation. Briefly, Ca^{2+} activates calcineurin that promotes the dephosphorylation of Nfat3 and its subsequent translocation to the nucleus, where it binds to Gata4 to promote pro-hypertrophic genes. Transgenic mice that express active calcineurin or Nfat3 develop cardiac hypertrophy and dilated cardiomyopathy (14). Recently, the Gata4 chromatin occupancy in cardiomyocytes and heart endothelium was mapped during heart development. This study revealed that the occupancy of Gata4 has features in lineage-specific enhancers. In cardiomyocytes, the TF Nkx2-5 guides Gata4 to myocyte-specific enhancers, while in endothelial cells, the ETS proto-oncogene 1 (Ets1) brings Gata4 to endothelial lineage enhancers (15). Interestingly, the roles of Gata4 in the heart are numerous, but it has been shown to be crucial in maintaining cardiac homeostasis and development. Importantly, Gata4 has been shown to play both a pro- and anti-hypertrophic role in the heart, depending on which TF it is binding, and on which genes these complexes are found (13) (14).

Recently, a histone methyltransferase, G9a, was described as mediator of cardiac homeostasis. G9a represses embryonic gene programming in adult cardiomyocytes through H3K9me2, a mark of transcriptional repression. Interestingly, G9a interacts with the catalytic subunit of the polycomb repressive complex 2, Ezh2, to regulate Mef2c target genes in the heart (16). Another interaction partner of Mef2c is the histone deacetylase 4 (Hdac4), that represses Mef2c activity. Upon pressure overload Hdac4-deficient mice showed an over-activation of Mef2c that developed into aggravated hypertrophy (17).

Another epigenetic modulator affecting heart physiology and disease is the ATP-dependent chromatin-remodeling complex, in which multi-proteins with an ATPase subunit modulate the distribution of nucleosomes to make chromatin accessible to TFs. In the context of cardiac hypertrophy, the role of the BAF complex was highly studied in the past decade (18). This complex is abundant in developing hearts and downregulated in the adult myocardium to modulate the switch between embryonic myosin heavy chain (*Myh6*) and adult (*Myh7*). The BAF complex recruits some of the abovementioned proteins including G9a and HDACs (19).

Interestingly, the Nogo family of proteins have been recently implicated in the onset of cardiac hypertrophy and heart failure. The Nogo family of proteins are encoded by the *Rtn4* gene, and although several of these isoforms have been highly studied in the central nervous system, two main splice isoforms are expressed in the heart: Nogo-B in endothelial cells and Nogo-A in cardiomyocytes. Both isoforms are involved in the regulation of sphingolipid metabolism in the heart. Within sphingolipids, there is growing evidence that ceramides play a central role in the development of heart failure, in part by increasing autophagy and cell death. However, the mechanism by which elevated ceramides regulate autophagy in cardiomyocytes during pressure overload is largely unknown (21). Studies have shown that Nogo-B (endothelial) deficient mice subject to transverse aortic constriction (TAC) are resistant to hypertrophy, hypertension and inflammation (20). On the contrary, mice lacking Nogo-A in cardiomyocytes showed severe dilated cardiomyopathy, cardiac dysfunction and high mortality rate after pressure overload. Nogo-A acts as an inhibitor of the serine palmitoyltransferase (SPT) enzyme, which is the rate limiting enzyme for *de novo* sphingolipid synthesis. Mechanistically, in hypertrophic hearts, the loss of Nogo-A leads to an excessive activity of SPT, resulting in a ceramide accumulation in cardiomyocytes. This accumulation of ceramides suppresses “beneficial autophagy”, despite this mechanism is not well known, reduced autophagy triggers mitochondrial ROS production and impairs metabolic genes, leading to severe HF (21).

Finally, non-coding RNAs have become increasingly important in the study of cardiac homeostasis and cardiovascular disease, since more than 97% of the genome is untranslated. As such, understanding the mechanisms of regulation of the non-coding transcriptome will be crucial for the development of novel therapeutic targets (22).

In the last decade, an increased number of non-coding transcripts have been described in the onset of different cardiac pathophysiologies and in cardiac development, including miRNAs, and lncRNAs. miRNAs (≈20nt) target the 3'-untranslated regions of mRNA and suppress translation via an RNA interference mechanism (22). For example, miR-1 induction reduces hypertrophy in cultured neonatal cardiomyocytes and adult hearts by downregulating the mentioned TFs, namely Gata4, Mef2 or Nfat (23). miR-22 impairs Ca^{2+} loading in cardiomyocytes by suppressing peroxisome proliferator-activated receptor (*Ppar*), estrogen-related receptor (*Err*), sirtuin 1 (*Sirt1*), and HDACs (24) lncRNAs are a heterogeneous group of non-coding transcripts that are involved in a wide variety of functions within the cell, and through several molecular mechanisms. Their function is usually linked to their genomic position and orientation to their neighboring PCG: thus, they are classified as being sense, antisense, intergenic or bidirectional with respect to the nearby gene. Notably, among these, long-intergenic ncRNAs (lincRNAs) have been shown to frequently regulate their nearby gene (30). Around 20% of the known lncRNAs are present in the cytoplasm, where they regulate gene expression at the posttranscriptional level, for example, acting as a molecular sponge of miRNAs. Since more than 80% of the currently described lncRNAs are present in the nucleus, they mostly act as regulators of gene expression at the epigenetic or transcriptional levels, in either *cis* or *trans* (30).

lncRNAs, which are the main focus of this study, are a wide heterogeneous group of ncRNAs comprising non-coding transcripts with more than 200 nucleotides in length, that can regulate gene expression at the nuclear and cytoplasmic levels. lncRNAs affect all cell types of the heart and play a central role for the onset of CVD and heart development (30). One such example is *Chrf* (cardiac hypertrophy-related factor), that sponges miR-489 in TAC: *Chrf* is able to directly bind to miR-489 and regulate miR-498 targets including Myd88 (myeloid differentiation primary response gene 88), and decrease hypertrophy (31). Another heart-enriched lncRNA is *Chaer*, that interacts with the polycomb repressor complex 2 (*PCR2*), which catalyzes H3K27 di- and tri-methylation to repress transcription: *Chaer* interferes in the H3K27 methylation of pro-hypertrophic genes promoters, and interestingly, inhibition of *Chaer* in heart before, but not after, the induction of TAC significantly attenuates hypertrophy, acting as a epigenetic checkpoint for the progression of pathological remodeling. (32).

Some of the most relevant molecular mechanisms of action include **signal lncRNAs**, expressed at a specific time in response a stimulus, and interact with chromatin remodelers (e.g., histone methyltransferases) to regulate transcription by modifying chromatin structure (33). **Decoy lncRNAs** bind transcription factors or other regulatory factors to repress transcription (34). **Guide lncRNAs** bind to transcription factors and carry them to their target site (33). **Enhancer lncRNAs** (eRNAs) are *cis*-acting transcripts that promote transcription of the nearby PCG, and they are transcribed from an active enhancer (35). Finally, **scaffold lncRNAs** can bring two proteins together to interact or be a functional part of a ribonucleic protein (36).

lncRNAs are poorly conserved in genomic sequence between species, however, recent studies have shown that the secondary structure, and therefore molecular function, is more conserved. Unfortunately, the current algorithms for secondary structure prediction are not accurate, as they predict secondary structures based only on minimum free energy (37). Conservation by synteny has arisen as the most robust method for identifying orthologs, especially for lincRNA, whose function is strongly associated to their genomic position. Synteny refers to the linear and ordered conservation of neighboring *loci* among species, indicating that syntenic conservation of the genes surrounding the lincRNA are indicators of orthology (38).

Therefore, in this study, we aim to better understand the role of non-coding RNAs in cardiac hypertrophy and heart failure. Using a mouse model of pressure overload, TAC, we screened for cardiac-specific lncRNAs dysregulated in hypertrophic ventricular cardiomyocytes. We identified more than 150 lncRNAs modulated 7 days after

aortic banding in mice. Furthermore, we characterized a lincRNA called *Chheaf-1*, a cardiac enriched lincRNA that regulates its nearby gene, *Rtn4*. Using a constitutive murine KO for *Chheaf-1* (*Chheaf-1*$^{-/-}$), we found that in the absence of *Chheaf-1*, mice have deficient levels of Nogo-A protein, deficient levels of autophagy-related markers, and present with a severe decrease of cardiac function after pressure overload, hypothesizing that *Chheaf*-1 plays a protective role in the heart. Finally, we identified a human ortholog for *Chheaf-1*, that follows the same pattern of expression in failing human hearts. Our study reveals a novel mechanism of epigenetic regulation of Nogo-A, via the lncRNA *Chheaf-1*, providing a potential new therapeutic target in the regulation of cardiac hypertrophy and failure.

MATERIALS AND METHODS

Animal experiments, echocardiography, cardiomyocyte isolation, Chheaf-1$^{-/-}$ generation.

All experiments were performed according to the 2010/63/EU Directive and approved by the ethics committee of Humanitas Research Hospital. Mice resided in a close environment with 12-h light/dark cycle and provided with chow diet after weaning. All experiments were carried out using 8 weeks old C57BL/6N mice. Langerdorff digestion was used for cardiomyocyte isolation as described elsewhere (39). For echocardiography, Vevo 2100 high-resolution digital imaging platform (VisualSonics) was chosen, using techniques previously described (40). First exon of the *Chheaf-1* transcript was cleaved using crispr-cas9 technology to generate a constitutive knock-out *Chheaf-1*$^{-/-}$ (41) mutant mice exhibited normal fertility and mendelian inheritance (data not shown).

Minimally invasive TAC.

At 8 weeks of age, *Chheaf-1*$^{-/-}$ and WT mice were subjected to sham or TAC operation as reported elsewhere. (42) Briefly, in anaesthetized mice with ketamine/xylazine (100/5 mg/kg) aortic arch was exposed after a horizontal incision at the level of the second intercostal space. A 26-gauge needle was used and rapidly removed after having tied a 7-0 nylon ligature between the innominate and left common carotid artery, producing an arterial stenosis. Sham-operated mice were subjected to the same procedure without the aortic ligation.

Myocardial screening of lncRNA by RNA-seq

Two biological replicates were profiled at each experimental point. RNA was isolated using the RNeasy Mini Kit (Qiagen) and treated with DNase according to the manufacturer's protocol. Total RNA quality was evaluated with a 2100 Agilent Bioanalyzer and the RNA 6000 Nano kit: only samples with RIN score >7 were further processed. RNA-seq libraries were created using the ScriptSeq Complete Gold - Low Input kit. Paired end sequence reads (50 bp in length) were generated on an Illumina HiSeq 2000. The correlation coefficient of the transcriptome between duplicates at the same experimental point ranged from 0.97 to 0.99, indicating strong reproducibility of the technique in our hands. The sequencing reads were processed to remove Illumina barcodes and aligned to the UCSC Mus musculus reference genome (Ensembl GRCH38), using Star v2.5. ReadsPerGene.out.tab files were then processed with edgeR. The RNA expression level of a gene was calculated in reads per kilobase per million mapped reads (RPKM) considering the sum of exon length. Differentially expressed coding and non-coding genes were selected based on the following parameters: FDR ≤0.05, RPKM ≥1 in at least one biological condition and coefficient variation among replicates below 100%. To evaluate tissue enrichment, complete raw data from mouse Encode projects were downloaded and analyzed using the same strategies described above.

Myriocin treatment in mice following TAC.

At 8 weeks of age *Chheaf-1*$^{-/-}$ and WT mice were subjected to sham or TAC operation, then intraperitoneally injected with myriocin (My, 0.1 mg/kg, #M1177; Sigma, St Louis, MS, USA) in 0.4% fatty acid–free bovine serum albumin (BSA) in phosphate-buffered saline (PBS) or vehicle. Mice were injected at day 1, 3 and 5 after surgery as previously reported (21). 7 days after surgery echocardiography parameters were registered and mice were sacrificed for cardiomyocyte isolation and further analysis by western blot and RT-qPCR.

Cell culture.

HL-1 cardiomyocyte cell line was cultured using Claycomb medium (51800C, Sigma) supplemented with 10 % fetal bovine serum (TMS-016-B, Sigma), 1 % penicillin-streptomycin (Invitrogen), 1 % ultra-glutamine (Invitrogen), and 0.1 mM norepinephrine (A0937-5G, Sigma), following Claycomb laboratory protocol for maintaining these cells in culture.

GapmeR knockdown or Chheaf-1 overexpression, Gata4 knockdown and p300 inhibition

Transient silencing of *Chheaf-1* with GapmeR/scramble in HL-1 cells was performed using lipofectamine 200 (Invitrogen) for 12h. 100 nM or either scramble or GapmeR was used. Cells were collected 24h after transfection for RT-qPCR analysys, western blot or ChIP. LNA GapmeR_*Chheaf-1* (Qiagen) 5'-GTGTCAGGAGAATGGT-3' LNA Scramble GapmeR_scramble sequence (Qiagen) 5'-AACACGTCTATACGC-3'

For overexpression, 80 ng of either *Chheaf-1* pcDNA3 vector or empty pcDNA was used, the transfection happened with lipofectamine 200 (Invitrogen) for 12h, cells were collected 24h after transfection for RT-qPCR analysys, western blot or ChIP. *Gata4* was silenced using siGata4 (#SASI_Mm01_00025092, Sigma) at concentration of 100nM with lipofectamine for 12h, cells were collected 24h after transfection for RIP experiments. p300 inhibition was achieve with C646 (SML0002-25MG, Sigma) compound, treatments were performed in serum-starved cells (overnight) at 25 μM for 24h, cells were collected for ChIP.

Chromatin immunoprecipitation (ChIP)

ChIP protocol was performed as previously described (43), briefly, chromatin was sonicated and immunoprecipitated overnight at 4°C with Anti-Histone H3 antibody (ab176842, abcam) anti-H3K27ac (ab4729, abcam) antibody. Primers for ChIP: *Chheaf-1* promoter (5'-TTTGACAGTTCTGCATGCCC-3'and 5'-GGATTTTATGACTGTGGGGCC-3') *Chheaf peak 2* (5'-AGTCCATGCTTCCGTCTTGA-3' and 5'-AGGAGCACAAAGTCAGACCC-3') *Rtn4* promoter (5'-CCCGCTTTCAAGTACCAGTT-3' and 5'-CTCCAGCACCTCCAATTCCT-3') Control 100Kb *Rtn4* 5'-AGAACTTCGGGCAGTACACA-3' and 5'-TGACCATCCAGCCAATCCAT-3') Xirp (5'-CCTTGGATGCCACTATGAGAAT-3' and 5'-GAATCCAATTCTGCCTCTCATC-3')

Cell Sorting

After Langerdorff digestion, cardiomyocytes were purified using an autofluorescence approach (44), while the other cells types were sorted in the BD FACSAria™ III sorter using antibodies, namely CD45 (564225, BD Horizon) for immune cells, CD31 (562861, BD Horizon) for endothelial cells, CD140a (25-1401-82, Invitrogen) for fibroblast and CD146 (740636, BD Horizon) for pericytes.

RNA extraction, RT-qPCR and ddPCR

RNA was extracted using RSC Maxwell simplyRNA Cells Kit (Promega, Madison, WI, US) and quantified using NanoDrop 8000 (Thermo scientific) spectrophotometer, then RNA was reverse-transcribed using Super Script VILO cDNA Synthesis Kit (Invitrogen). cDNA was measured by RT-SYBR green master mix (Applied Biosystem) or by ddPCR using QX200 AutoDG Droplet Digital PCR System (Bio-rad) Primers: **mice:** *HPRT* (5'-TCCTCCTCAGACCGCTTTT-3' and 5'-CCTGGTTCATCATCGCTAATC-3') *Chheaf-1* (5'-TCTTGAATGCTCCAGCTCACA-3'and 5'-CTCCGAAGCTCCTCCTGTAGA-3') *Rtn4* (5'-AGACCCTTTTTGCTCTTCCTG-3' 5'-TGTTACCTGGCTGCTCCTTC-3') *Ccdc88a* (5'-GAGACGCTCAGAGAGAATTCAG-3'and 5'-ACTAATCTGGGAGCGCTGC-3') *Star* (5'- GGGCATACTCAACAACCAGG-3' and 5'-AAACACCTTGCCCACATCTG-3') *Cnn1* (5'-CGGGAACAACTTCATGGATGG -3'5'-TCTTCACAGAACCCGGCT-3')*Rbsm3* (5'-TACATTCCCCAGTACACGCC -3'and 5'- GCTAACTGTTGCTGCTGACC-3') *Serpinb1a* (5'- GTGAGCAAACGTGGAGCATC-3'and 5'- GGGCCAAGTCAGCACCATA-3') **human:** *hCHHEAF-1* 5'-GCAGGCAGATGACTTGAGGT-3' and 5'-CACCGTGCCCACCTAATTTT-3') *RTN4A/B* 5'-GCAGAGCTGAGTAAAACTTCAG-3' and 5'-GTTCACATGACCAAGAGCAG-3') *18S* (5'-CGCAGCTAGGAATAATGGATAAGG-3' and 5'-CATGGCCTCAGTTCCGAAA-3')

RNA sequencing in Chheaf-1$^{-/-}$ vs. WT mice.

Three biological replicates of Langerdorff isolated cardiomyocyte at different times post-banding (at 1, 2 and 4 weeks after TAC) were sequenced. RNA-seq library preparation was performed with the SMARTer Stranded Total RNA-Seq Kit v2 - Pico Input Mammalian (Takara Bio), according to the manufacturer's instructions. Ribosomal

RNA was depleted using the RiboGone method included in the kit. Paired-end multiplexed libraries were sequenced using the NextSeq2000 instrument (Illumina, San Diego, US). An average of 250 million reads/sample were obtained. Paired-end reads of 75bp were aligned to the GENCODE Mus musculus reference genome (build GRCm38/mm10) using STAR v2.7.2b13. Raw read counts were normalized with TMM implemented in edgeR and lowly expressed genes were filtered out with the filterByExpr(min.count=20) function; differential expression analysis of read counts was performed using voom, lmFit and eBayes(robust=T) function of limma v.3.4652 package in R. Significant differential genes were chosen based on an FDR < 0.05 and |log2FC| > 0.5.

Western blot

Cardiomyocytes were isolated as previously reported from hearts of sham or TAC, or HL-1 cells were tripsinized and pelleted. WB was performed as reported elsewhere (45). Briefly, proteins were extracted from the cellular pellet using RIPA buffer (Radioimmunoprecipitation assay buffer) containing PMSF (#329-98-6, sigma) and protease inhibitor (#11873580001; Roche). SDS-PAGE was carried out using 20 µg of cell lysate. The following antibodies were used for WB analysis: NOGO-A/B (#AF6034; R&D Systems), GADPH (#2118, cell signaling) Autophagy Antibody Sampler Kit (#4445, cell signaling), GATA-4 antibody (#AB_2615046 active motif)

Northern Blot

RNA from either total LV or HL-1 cell pellet was extracted using PureZOL reagent (BioRad), then a total of 5 µg of RNA was depleted from rRNA using RNeasy Pure mRNA Bead Kit (#180244, Qiagen). Northern blot was performed as reported elsewhere (46) Briefly, RNA was run in a 1% agarose gel (1xMOPS buffer, 1% formaldehyde), transferred to a positive charged nylon membrane in 20X SSC buffer by capillarity and then crosslinked with UV fixation. Membrane was incubated with NorthernMax Pre-hybridization/Hybridization Buffer at the probe indicated temperature, and incubated overnight with DIG-conjugated probes in Hybridization Buffer at the probe temperature. Then membranes were washed in Northern blot low stringency buffer, Northern blot high stringency buffer and 1X PBS-Tween subsequently. Next membranes were blocked in blocking solution (Roche) in 1X PBS-T, and incubated overnight with α-DIG-HRP secondary antibody (1:2000) for 1 h at room temperature, finally membranes were washed three times with 1X PBS-T and developed with enhanced chemiluminescence.

RNA Immunoprecipitation (RIP)

As previously described (46) HL-1 cells were crosslinked using 150 mJ UV irradiation, then washed in PBS and collected by centrifugation. Pellet was lysed in RIP buffer on ice for 30 min and pellet collected by centrifugation, then pre-cleared with protein-G magnetic beads, nex, pre-cleared lysate was incubated with conjugated antibody-protein-G-bead complexes GATA-4 antibody (#AB_2615046 active motif). Finally, the complex Bead-antibody-lysate complexes was washed and RNA eluted using PureZOL isolation reagent (BioRad), followed by classical RNA extraction.

Statistics

All data are expressed as mean ± SEM, Gaussian distribution was confirmed using normality test, unpaired t-test was used to analyze two groups, ANOVA was used for experiments with more than two independent groups: ordinary one-way; for those with two between-subject factors: ordinary two-way, Tukey or Sidak was chosen for post-hoc analysis. Statistical analysis were performed by using GraphPad Prism software (version 8.0)

RESULTS

Myocardial screening of novel lncRNA transcripts in murine cardiomyocytes subjected to pressure overload

Over the last decade, many studies have revealed the importance of lncRNAs in various pathophysiologies including cancer and cardiac disorders. However, the study of such non-coding transcripts reveals great complexity as a result of their low expression, high cell-type specificity and scarce annotation. To overcome these layers of complexity and to discover novel lncRNAs with relevant roles in the development of cardiac hypertrophy, we performed whole genome RNA-sequencing in cardiomyocytes (CMs) of mice subjected to pressure overload (TAC). We then analysed the differential gene expression profile of cardiomyocytes at 1,2,4 and 7 days post-banding: at day 7, we found more than 150 lncRNAs differentially expressed (Fig 1A).

In order to select a promising candidate for our study, we filtered this list to identify a novel long non-coding RNA with therapeutic potential for cardiomyocyte hypertrophy. Therefore, we selected a set of lncRNAs that were oriented in an intergenic manner (lincRNA), cardiomyocyte specific and significantly upregulated after pressure overload. This filtering revealed several non-coding transcripts fitting these requirements. After *in vitro* validation of these lncRNAs (data not shown), we selected *Gm12092* as the top candidate for our study.

Gm12092, which we named *Cardiac and hypertrophy and heart failure-1* (*Chheaf-1*), is upregulated after TAC, reaching a peak of expression at 7 days post-surgery (Fig 1B, C). Interestingly, its expression decreases 2 weeks post-TAC to increase again after 4 weeks (Appendix S1A). Moreover, gene expression analysis confirmed that *Chheaf-1* is heart-enriched, predominantly in the left ventricle (LV) (Fig 1D). Furthermore, sorting all the cell populations of the left ventricle (44), we found that *Chheaf-1* is exclusively expressed in adult cardiomyocytes (Fig1E). To confirm the presence of *Chheaf-1* in cardiac cells, we performed Norther Blot analysis (Fig 1F) and 3' rapid amplification of cDNA ends (3' RACE) in murine left ventricle (Fig 1G) and HL-1 cells (Appendix S1B) for a complete annotation, and to map *Chheaf-1* transcription start sites. In fact, we found that *Chheaf-1* is present in the LV and annotated as a 600bp transcript.

Subcellular localization of biomolecules is important for their function, and therefore, performing subcellular fractionation, we determined that *Chheaf-1* is mostly present in the chromatin fraction of HL1 cardiomyocytes (Fig 1H). Therefore, we discovered *Chheaf-1*, a novel 600bp lincRNA, upregulated 7 days post-banding and enriched in cardiomyocytes from hypertrophic left ventricles.

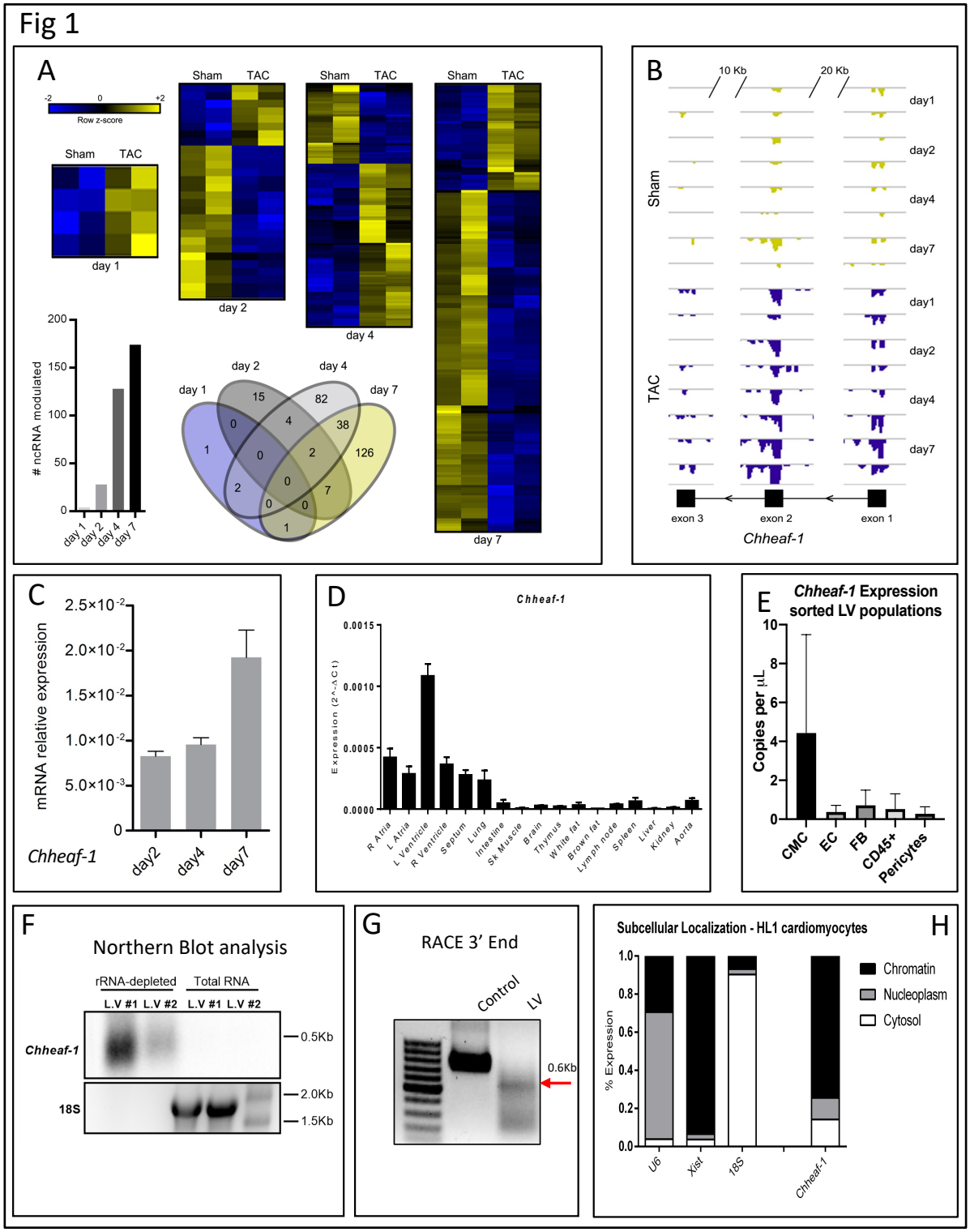

Figure 1. *Chheaf*-1 discovery, localization and annotation. (A)Heat map of lncRNAs differentially expressed from RNA-seq data of cardiomyocytes isolated from mice at 2, 4, and 7 days after TAC, lower left: Bar graph showing the number of non-protein coding genes modulated in TAC, lower centre: Venn diagram showing the number and overlap of modulated non-protein coding genes in TAC (B) Expression pattern of *Chheaf*-1 *locus* from RNA-seq of cardiomyocytes isolated from mice at 2, 4, and 7 days after TAC (C) RT-qPCR analysis of *Chheaf-1* expression from murine cardiomyocytes at 2, 4 and 7-days post-TAC. (D) RT-qPCR analysis of *Chheaf-1* in 17 different mouse tissues (G) *Chheaf-1* expression in sorted adult heart cell populations cardiomyocytes (CMC), fibroblasts (FB), endothelial cells (EC), immune cells (CD45+) and pericytes) (F) Northern blot using biotin probes for *Chheaf-1* in left ventricle with and without rRNA depletion, 18s was not observable in rRNA depleted samples (G) 3' RACE products run on a 1% agarose gel (H) HL1 cell fractionation (nucleoplasm, chromatin, and cytoplasm, as indicated) followed by RT-qPCR analysis. Controls include: *U6* (nucleoplasm) *Xist* (chromatin) and 18s (cytosol)

The loss of *Chheaf-1* aggravates pathological cardiac hypertrophy via *Rtn4* regulation.

lincRNAs often execute their function on their nearby gene: *Chheaf-1* is located in between two genes in an antisense trend, *Rtn4* and *Ccdc88a* (Fig 2A). To test whether *Chheaf-1* is regulating one or both of these genes, we used gain- and loss-of-function approaches using overexpression or a GapmeR (knockdown), respectively, in HL-1 cells (Fig 2B, Appendix S2A). Here, we reveal that *Chheaf-1* regulates *Rtn4* expression, as *Rtn4* increases when we overexpress *Chheaf-1,* and decreases after silencing with the GapmeR. Of note, it has already been reported that Nogo-A increases in cardiomyocytes after TAC (21), which we also observed (Appendix S2B). No effects in expression of *Ccdc88a* were found (Appendix S2C), thus it was not considered further for this study. Therefore, the main focus of this project is the regulation of *Rtn4* by *Chheaf-1.*

To assess the role of *Chheaf-1* in the heart, and whether it is involved in the regulation of *Rtn4,* we generated a constitutive KO mouse lacking exon 1, *Chheaf-1*$^{-/-}$ (Fig2C). We evaluated the cardiac function of these mice for a period of 8 months at the basal level, and we did not observe any changes in cardiac function in the wild-type vs. the knockout mice (Fig2D). KO mice were subjected to TAC, and cardiac function was assessed at 1, 2, and 4 weeks post-surgery. Interestingly, *Chheaf-1*$^{-/-}$ subjected to TAC had a significant decrease in cardiac function in comparison with the WT TAC mice, namely seen by a decrease in ejection fraction (EF) (Fig2E) and fractional shortening (FS) (Appendix S2D), indicating that the aortic constriction produces a worse outcome in hearts lacking *Chheaf-1*. We observe no effects of *Chheaf-1*$^{-/-}$ cardiac function in the sham operated mice (Fig2E). These data altogether provide evidence that upon pressure overload, the increase of *Chheaf-1* expression has a protective effect on the heart. Given that in the absence of *Chheaf-1,* we observe a severe loss of cardiac function under pressure-overload conditions, we can conclude that it is necessary for protecting the heart against pathological hypertrophy and progression to heart failure.

In order to fully understand the role of *Chheaf-1* in the regulation of cardiac hypertrophy and HF in mice, we carried out a whole-genome RNA-sequencing of cardiomyocytes isolated from *Chheaf-1*$^{-/-}$ and *Chheaf-1*$^{+/+}$ mice at 1, 2, and 4 weeks after TAC (Fig1F). Interestingly, after a differential gene expression analysis, we found that only 5 genes were significantly dysregulated 1 week after TAC, including *Star*, *Cnn1*, *Rbsm3* and *Serpinb1a* and *Rtn4*. This suggests that the decrease in cardiac function in *Chheaf-1*$^{-/-}$ mice is due to *Rtn4* downregulation. Of note, we observe an increase in Nogo-A expression in wild-type TAC mice versus the wild-type Sham group, an effect which is completely blunted in *Chheaf-1*$^{-/-}$ cardiomyocytes: in the absence of *Chheaf-1*, Nogo-A expression is not induced after pressure overload (Fig2G). This further confirms our hypothesis that *Chheaf-1* regulates Nogo-A, an effect which we confirmed *in vitro* by silencing or overexpressing *Chheaf-1:* Nogo-A is down- or up-regulated, respectively, in HL-1 cardiomyocytes (Appendix S2A). We observed no changes in *Star*, *Cnn1*, *Rbsm3* and *Serpinb1a* expression following either knockdown or overexpression of *Chheaf-1* in HL1 cardiomyocytes (Appendix S2E), confirming the hypothesis that the cardiac phenotype we observe in *Chheaf-1*$^{-/-}$ mice is a result of its regulation of *Rtn4*.

Given that in cardiac endothelial cells, loss of *Rtn4* (Nogo-B) has a protective effect on the heart after pressure overload (20), we evaluated the expression of *Rtn4* in cardiac endothelial cells of *Chheaf-1*$^{-/-}$ vs *Chheaf-1*$^{+/+}$ mice in sham vs. TAC conditions. We did not observe changes in *Rtn4* expression (Appendix S2F) nor in blood pressure (data not shown), likely due to the low (if negligible) expression of *Chheaf-1* in this cellular compartment, therefore excluding the effect of *Chheaf-1* in other cell populations of the heart.

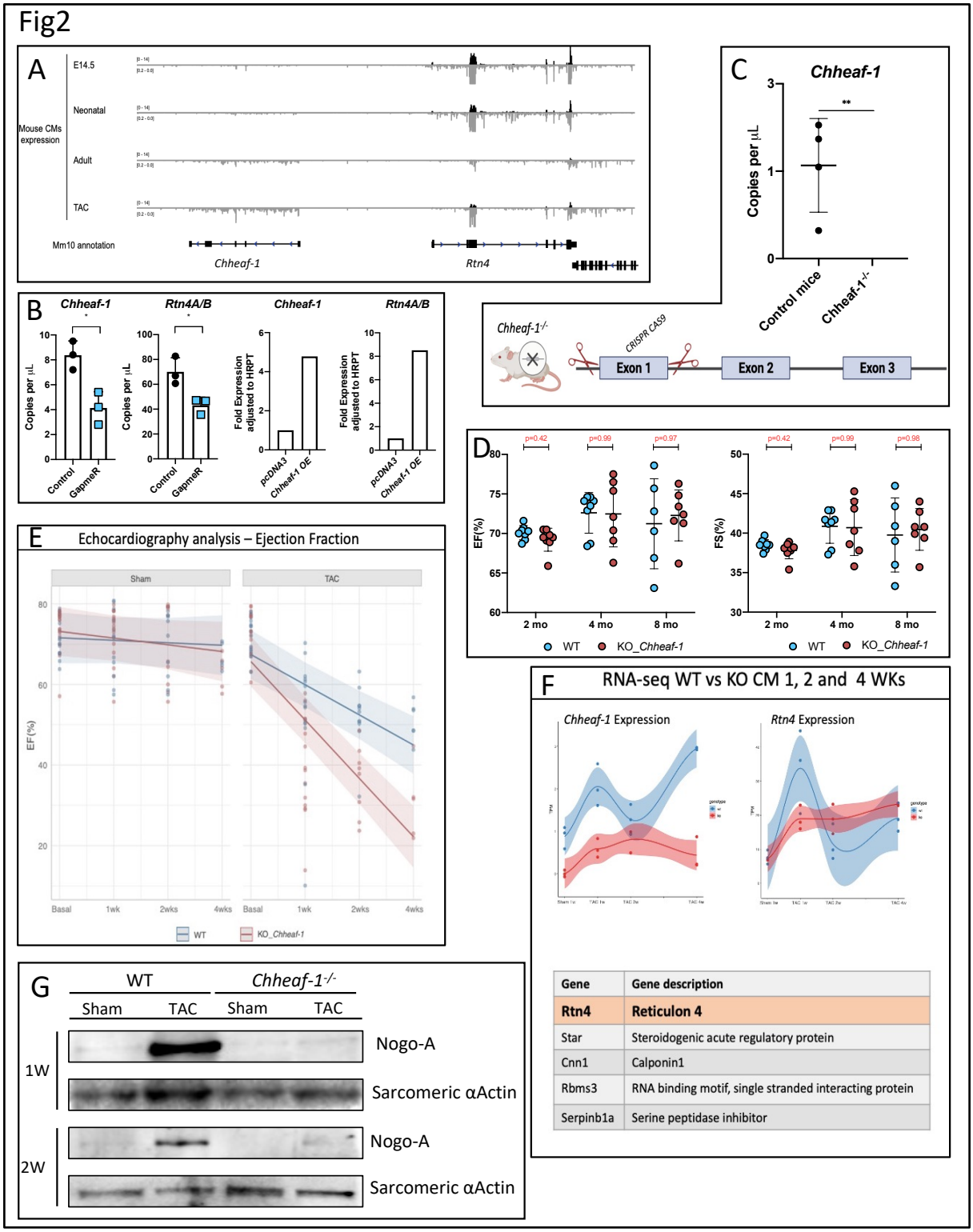

Gene	Gene description
Rtn4	**Reticulon 4**
Star	Steroidogenic acute regulatory protein
Cnn1	Calponin1
Rbms3	RNA binding motif, single stranded interacting protein
Serpinb1a	Serine peptidase inhibitor

Figure 2. *Chheaf-1* regulates cardiac function through *Rtn4*. (A) RNA-seq bigwig profile of *Chheaf-1* & *Rtn4* loci at E14.5, neonatal, adult and TAC. (B) RT-qPCR analysis of HL-1 cells treated with either GapmeR or overexpression, unpaired t-test analysis was used (p=0.013) (C) Schematic representation of the *Chheaf-1* constitutive KO line generated with Crispr-Cas9, and ddPCR analysis confirming *Chheaf-1* genomic cleavage. Unpaired t-test was used (p=0.0017) (D) Echocardiography parameters: EF and FS of mice followed for 8 months, one-way ANOVA with Sidak post-hoc test was used (E) Interaction plot of echocardiography parameters: EF of *Chheaf-1*$^{-/-}$ vs. WT subjected to Sham (left) or TAC (right) (F) Expression of *Chheaf-1* and *Rtn4* and differential gene expression analysis 1W after TAC from RNA sequencing data of WT vs. KO CM at 1,2,4 Weeks after TAC (G) Western blot of *Chheaf-1*$^{-/-}$ CMs after 1W and 2W TAC vs Sham.

***Chheaf-1* regulates autophagy through Nogo-A**

It has previously been shown that the absence of Nogo-A in cardiomyocytes aggravates the hypertrophic outcome after pressure overload. Nogo-A inhibits the activity of SPT-1, the rate-limiting enzyme for *de novo* sphingolipid synthesis. In the absence of Nogo-A in TAC mice, the activity of SPT-1 is restored, leading to a disproportionate synthesis of sphingolipids. Hence, cardiomyocytes accumulate an excess of sphingolipids, mainly ceramides. Upon pressure overload, sphingolipid accumulation prevents cardiomyocytes from entering into a beneficial autophagy phase, thus aggravating cardiac function and the hypertrophic response (21).

In order to evaluate whether *Chheaf-1*$^{-/-}$ mice present with the same dysregulation of autophagy after pressure overload, we measured the protein levels of well-known autophagy markers. Intriguingly, at basal levels, we observed an absence of these markers in *Chheaf-1*$^{-/-}$. Moreover, there is a reduction of autophagy markers in *Chheaf-1*$^{-/-}$ TAC mice in comparison with the WT TAC controls at both 1- and 2-weeks post-surgery (Fig3A). This leads us to hypothesize that, just as in the Nogo-A knockout, the absence of *Chheaf-1* results in a bypass of the protective autophagy stage upon pressure overload. We therefore believe that the exacerbated response to pressure overload in *Chheaf-1*$^{-/-}$ mice is due to deficient protective autophagy activation coupled to Nogo-A downregulation, however further studies are required.

To confirm that the loss of *Chheaf-1* enhances ceramide accumulation and supresses protective autophagy in hypertrophic hearts, we treated *Chheaf-1*$^{-/-}$ mice with myriocin (Myr, 0.1 mg/kg i.p), at days 1-, 3- and 5-days post-TAC surgery. Myriocin is a potent SPT inhibitor, that blocks the *de novo* synthesis of sphingolipids and thus prevents ceramide accumulation. Interestingly, myriocin was able to restore not only cardiac function (Fig3B), but classical autophagy markers in cardiomyocytes of *Chheaf-1*$^{-/-}$ mice 1-week post-TAC (Fig3C). No changes in WT and Sham mice were observed, as previously published (21). Myriocin does not affect gene expression of *Chheaf-1* or *Rtn4* (Fig1D). Similar results were obtained in a Nogo-A KO mouse model (21). These results indicate that *Chheaf-1* is needed to prevent ceramide accumulation in cardiomyocytes after TAC, via *Rtn4* regulation.

.

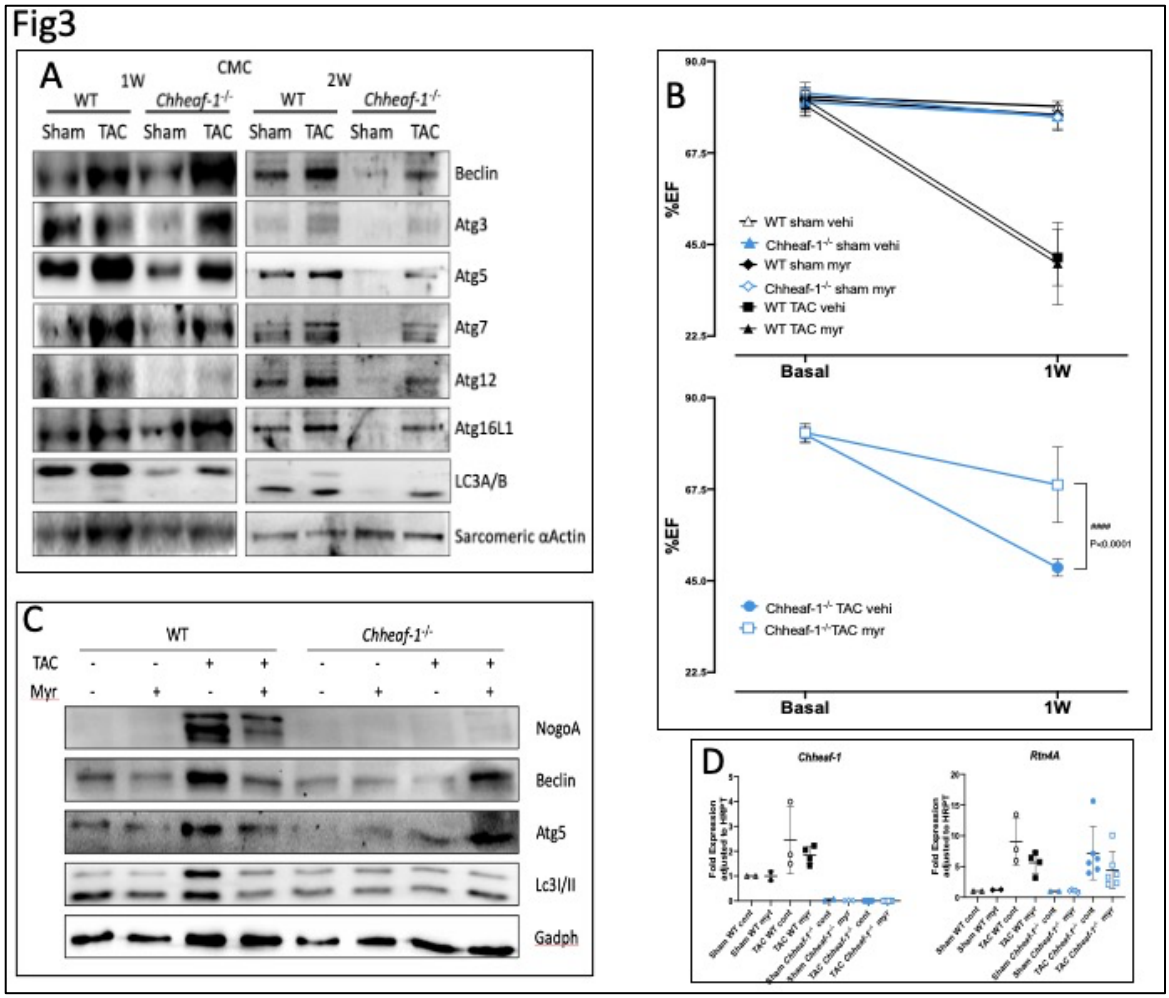

Figure 3: *Chheaf-1*$^{-/-}$ mice have reduced levels of autophagy markers upon TAC that are restored concomitantly with cardiac function after Myriocin (Myr) treatment: (A) western blot assessing classical autophagy markers, as indicated. (B) Cardiac function assessed by echocardiography **Upper:** %EF of Myriocin treated/non-treated WT and *Chheaf-1*$^{-/-}$ 1 week after sham or TAC **Bottom**: %EF of Myriocin treated/non-treated *Chheaf-1*$^{-/-}$ mice 1 week after TAC. Two-way Anova was used with Sidak post-hoc test, p<0.0001. (C) Western blot assessing autophagy markers in Sham/TAC *Chheaf-1*$^{-/-}$ vs control CMC, as indicated. (D) RT-qPCR analysis of CMC from WT vs *Chheaf-1*$^{-/-}$ mice 1 week after TAC treated with either Myr or vehicle.

Chheaf-1 regulates H3K27Ac in the promoter region of *Rtn4* and its own *locus*

Chromatin state is critical for the maintenance of gene expression patterns: in fact, changes in chromatin state strongly affect cardiomyocytes during the onset of hypertrophy (9). Changes in chromatin structure are governed by histone modifications (among others), and following cardiac stress. Such modifications permit the switch between relaxed and condensed states of the chromatin, thus exposing or preventing promoters of pro- or anti-hypertrophic genes for transcription factor binding, respectively.

It Is known that chromatin-associated lincRNAs such as *Chheaf-1* often regulate histone modifications and/or interact with transcription factors. After a bioinformatic analysis comparing public ChIP-sequencing databases (16) of different histone modifications from TAC vs. Sham cardiomyocytes, we identified that the promoter of not only *Rtn4,* but *Chheaf-1,* are highly enriched in H3K27Ac (mark of activated transcription and active enhancers). Using chromatin immunoprecipitation to validate these observations in our model, we found a reduction of H3K27Ac in the promoter region of *Rtn4* and in the *Chheaf-1* locus in *Chheaf-1*$^{-/-}$TAC mice compared to the TAC WT controls (Fig4). Thus, we provide ulterior evidence that *Chheaf-1* regulates the transcription of *Rnt4* at the level of histone modifications (Fig4). This observation was also confirmed in gain- and loss-of-function assays in HL-1 cells (Appendix S3). These results altogether suggest that *Chheaf-1* plays a protective role on the heart through the epigenetic regulation of *Rtn4*

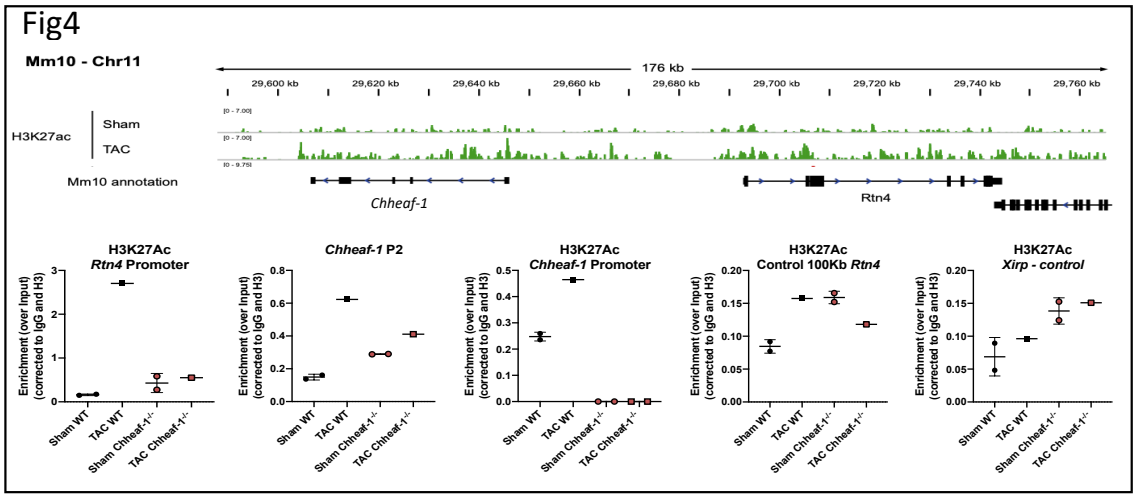

Figure 4. *Chheaf-1* regulates H3K27AC in the promoter region of *Rtn4*: **Upper**: Bigwig screenshot from public ChIP-seq data of H3K27Ac in sham vs. TAC CMCs in the promoter region of *Rtn4* and *Chheaf-1* **lower:** ChIP performed in CMCs of 1W TAC *Chheaf-1*$^{-/-}$ vs control mice, followed by RT-qPCR analysis of H3K27Ac enriched regions in *Rtn4* promoter and *Chheaf-1* locus (P2). Controls: *Chheaf-1* promoter, absent in the *Chheaf-1*$^{-/-}$ mice. 100Kb upstream of *Rtn4* promoter and *Xirp* heterochromatin control.

Potential Mechanism: *Chheaf*-1 interacts with Gata4 to regulate p300/Gata4-mediated H3K27Ac deposition

Transcription factors are known to be essential mediators for the pathophysiology of the heart. A very well-known mechanism is that of the pro/anti hypertrophic transcription factor Gata4, and the p300 histone acetyl transferase (9). p300 mediates the deposition of H3K27Ac and activates Gata4 to promote hypertrophic gene expression in cardiomyocytes (9). We previously reported that *Chheaf-1*$^{-/-}$ mice subjected to aortic banding have reduced levels of H3K27Ac in the promoter region of *Rtn4.* Moreover, a large number of lncRNAs present in the chromatin compartment are bound to either chromatin, transcription factors or both. Thus, in order to understand whether *Chheaf*-1 plays a role in regulating this canonical pathway, we first assessed the levels of Gata4 in *Chheaf-1*$^{-/-}$ mice after TAC. Surprisingly, *Chheaf-1*$^{-/-}$ mice have reduced levels of Gata4 in basal (sham) conditions. Moreover, we observe a reduction of Gata4 expression in the TAC KO in comparison to the TAC WT controls (Fig5A). Interestingly, levels of Gata4 mRNA do not change in these conditions (data not shown). This led us to hypothesize that *Chheaf-1* is regulating the stability of Gata4, potentially through a direct interaction. To this end, we performed RNA immunoprecipitation in HL-1 cardiomyocytes, and we confirmed a direct interaction (Fig 5B). Therefore, these data suggest that *Chheaf-1* is regulating *Rtn4* expression through the modulation of Gata4 activity, although further study into this mechanism is required.

In order to corroborate these data, we used a specific inhibitor of p300 (C646) to determine its effect on *Rtn4* transcription activation. Using chromatin immunoprecipitation, we observed that upon p300 inhibition in HL-1 cells, enrichment of H3K27Ac at the *Rtn4* promoter and *Chheaf-1* loci decreases (Fig5C). Therefore, these data suggest that *Chheaf-1* could be involved in the Gata4/p300 complex regulation, either by promoting the interaction between these two transcription regulators, or by recruiting this complex to the promoter region of *Rtn4* (Fig 5D), establishing *Chheaf-1* as a potent epigenetic mediator for the heart failure.

Fig5.

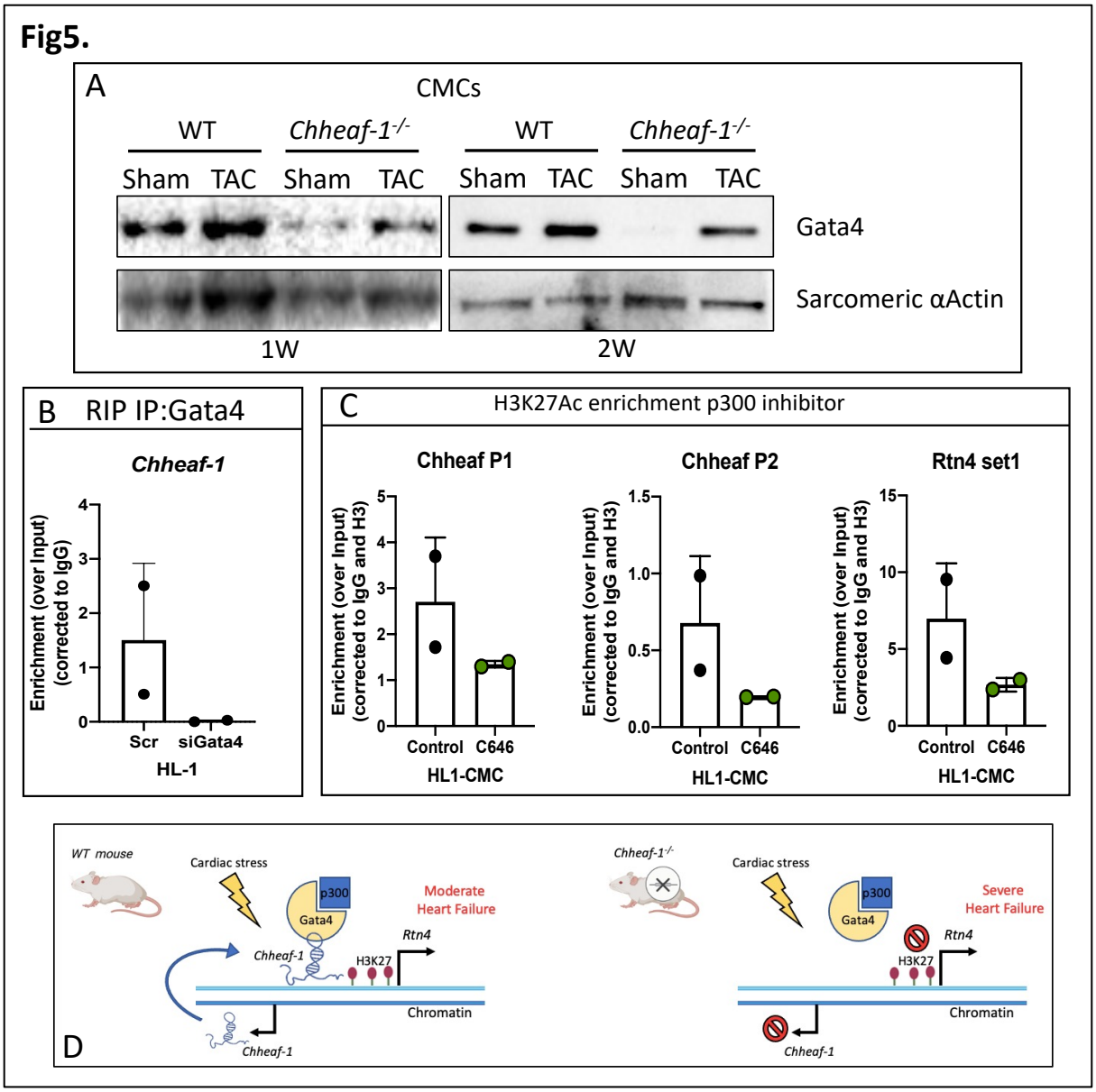

Figure 5: Hypothesis: *Chheaf-1* interacts with *Gata4* and recruits the Gata4/p300 complex to increase H3K27Ac in the *Rtn4* promoter region:(A) western blot of Gata4 in *Chheaf-1*$^{-/-}$ TAC/sham mice vs control. (B) RNA immunoprecipitation of Gata4 in HL-1 cells, followed by RT-qPCR analysis. siGata4 was used as an internal control. (C) ChIP-qPCR analysis performed in HL-1 cells treated with C646 (p300 inhibitor). Chromatin was immunoprecipitated with an antibody against H3K27Ac, and its enrichment was evaluated in the regions of *Rtn4* and *Chheaf-1 loci* (P1 and P2) (D) Graphical abstract of *Chheaf-1* regulating *Rtn4* through Gata4/p300.

Discovering the human orthologue: using epigenetic marks to decipher *hCHHEAF-1*

Finding a human orthologue of a lncRNA is currently one of the biggest challenges of this field, since these molecules are poorly conserved between species. Regardless of the poor conservation at the level of genomic sequence, the function of lncRNAs is often conserved beyond the DNA sequence (38). We therefore searched for lncRNAs in the syntenic region of *Rtn4* and *Chheaf-1* in human. In order to do so, we analysed public ChIP-sequencing data derived from patients with failing hearts (48) and we detected an increase of H3K27Ac in the human syntenic region of *RTN4* and *hCHHEAF-1*, mimicking the observed enrichment in mice (Fig 4,6). We then annotated the lncRNA using public RNA-sequencing data derived from HCM patients (49).

Using this annotation, we identified a single intergenic antisense lincRNA with respect to *RTN4*, matching the genomic features found in murine *Chheaf-1* (Fig6A).

In order to characterize *hCHHEAF-1* and see if it mimics the expression patterns of the mouse ortholog, we measured its expression in HF heart samples. We found that not only *RTN4,* but *hCHHEAF-1* are upregulated in right atria from failing hearts vs control hearts (Fig6B). Further characterization of this lncRNA is required in order to confirm its function and regulation of *RTN4.* Doing so will increase the translational value of our findings, as this lncRNA could be a potent therapeutic target for heart failure.

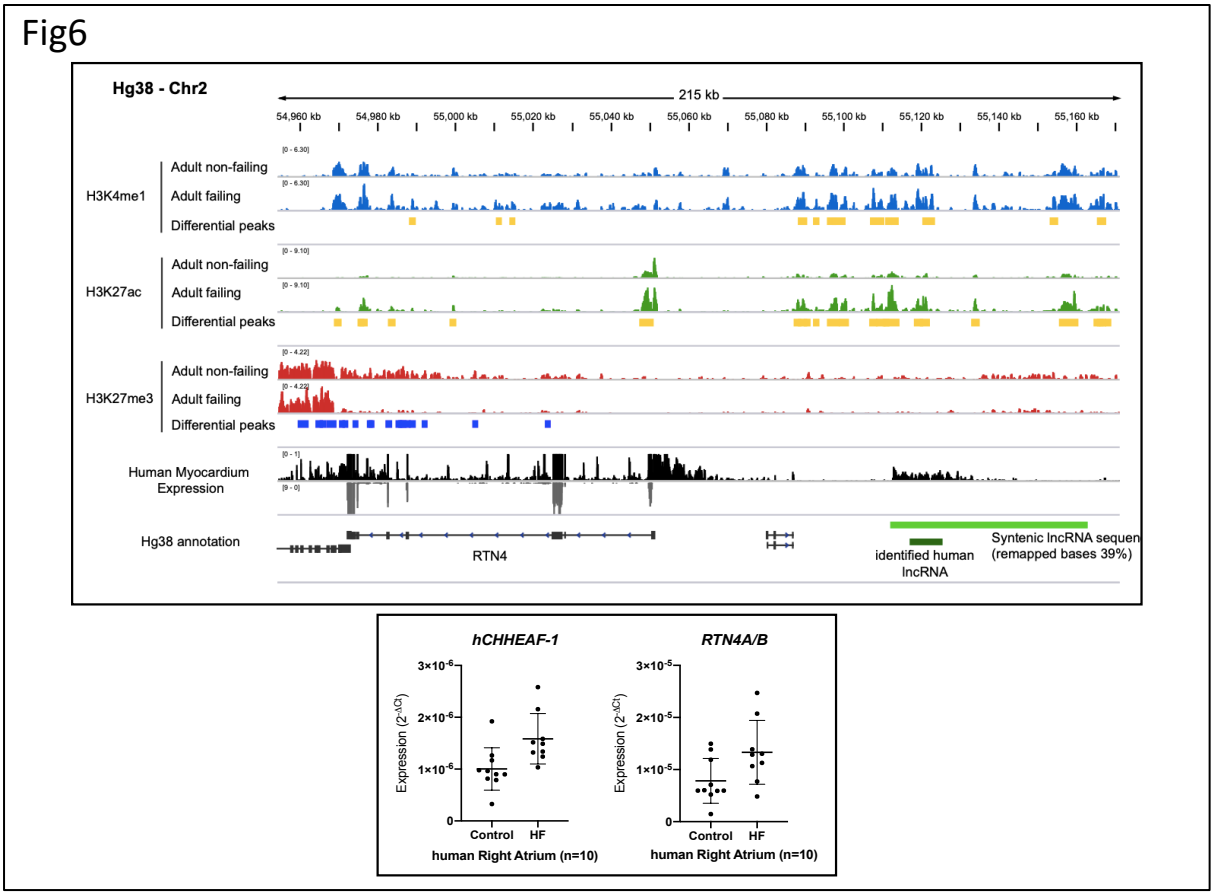

Figure 6. h*CHHEAF-1* human ortholog of *Chheaf-1*: (A) three first lanes: Screenshot of bigwigs showing the genome-wide distribution of H3K27ac analysed by ChIP-seq in cardiomyocytes from patients with failing vs. non-failing hearts **Fourth lane**: Bigwig from RNA-seq data of the human myocardium transcriptome of hypertrophic cardiomyopathy (HCM) patients **fifth lane**: Syntenic region of *Chheaf-1* in human and annotated lincRNA from HCM patients. (B) RT-qPCR analysis on RNA from human right atrium of failing hearts adjusted to 18s.

DISCUSSION

Even though cardiac hypertrophy is one of the main risk factors for the development of heart failure, the epigenetic mechanisms underlying this disease are, to date, largely unknown. In order to gain a better understanding of these mechanisms in HF, we discovered more than 150 novel lncRNAs dysregulated in cardiomyocytes upon pressure overload. Therefore, this study aimed to reveal the mechanism of a specific lincRNA, *Chheaf-1*, that is upregulated upon cardiac stress in cardiomyocytes and that has a protective effect on the heart.

Chheaf-1 enhances the expression of *Rtn4* in response to pressure overload, thus influencing Nogo-A downstream processes by avoiding ceramide accumulation and promoting beneficial autophagy. Interestingly, *Chheaf-1* is present in the chromatin compartment of cardiomyocytes and interacts with the transcription factor Gata4. The Gata4/p300 axis has been studied extensively in the context of cardiac hypertrophy: p300 is a histone acetyl transferase, that has the ability to modify the acetylation of the Histone 3 K27 residue, thus modulating chromatin structure by relaxing its conformation to make promoters accessible for transcription factors (7). Our results suggest that *Chheaf-1* is involved in this pathway, however we are currently investigating whether or not *Chheaf-1* binds to chromatin to recruit Gata4/p300 to the promoter region of *Rtn4*. In line with our work, the lncRNA *Khps1*, was shown to form a DNA/RNA triplex with the SPHK1 (proto-oncogene) promoter which is necessary for the recruitment of CBP/p300 (52). Moreover, the lncRNA *NppA-AS1* was shown to be involved in the recruitment of p300/Gata4 to the promoter of *NppA* to promote hypertrophy in cardiomyocytes (53). It is well known that Gata4 is a main transcription factor (together with Gata6) involved in cardiac development (54). We found that *Rtn4* is highly expressed at the embryonic stage, with a re-activation of expression after pressure overload. On the contrary, *Chheaf-1* expression in prenatal hearts is absent, and we did not observe any defects in cardiac development or embryonic lethality in the absence of *Chheaf-1*. This emphasizes that *Chheaf-1* plays a role only after pressure overload, and that the absence of *Chheaf*-1 drives the heart to severe failure.

Based on our data, we believe that the severe heart failure observed in our *Chheaf-1*$^{-/-}$ mice is, at least in part, due to the insufficient protective autophagy occurring in the cardiomyocytes. This reduced autophagy is a result of the regulation of Nogo-A, and its downstream effects on *de novo* sphingolipid synthesis and ceramide accumulation. It is known that autophagy occurs in the heart at low levels to maintain cardiac homeostasis, however it has been shown to be upregulated after pressure overload, and is linked to ceramide accumulation (55). Whether autophagy is beneficial or detrimental for the heart is still under debate, but excessive or deficient levels of autophagy are harmful for the proper functioning of the heart. In contrast to our hypothesis, others groups have shown that reduced levels of autophagy are favourable against cardiac stress, but in the context of lipotoxicity, as opposed to pressure overload (56). We are still investigating whether *Chheaf-1* is responsible for ceramide accumulation and changes in sphingolipid metabolism through its regulation of *Rtn4*, in order to fully understand its mechanism of action.

lncRNAs have been described as a new and powerful therapeutic strategy in the last decade, since many studies have focussed on lncRNA modulation *in vivo* demonstrating their ability to regulate cardiac dysfunction or reduce disease progression (57; 58; 59). Given the necessity for novel therapeutic targets of heart failure, modulation of lncRNAs using knockdown or overexpression could be promising.

GapmeRs have emerged as a new class of antisense oligonucleotides (ASO) used to knockdown nuclear lncRNA. They are built of a DNA core flanked by two locked nucleic acids (LNA) that allows them to enter into the nucleus, in contrast to siRNAs that act mostly in the cytoplasm. Currently, there are less than 10 drugs using ASO technology approved by the FDA, and only 25 are in phase III of clinical trials: all of these drugs target mRNA or miRNA, not lncRNAs (60). This is not only due to the novelty of lncRNAs, but the fact that hepatotoxicity has been reported with use of LNA oligonucleotides (61). On the other hand, overexpressing lncRNA presents an even more challenging approach, as it requires the use of viral gene delivery, nanoparticles, or RNA mimics. These three approaches cannot always efficiently overexpress the lncRNA, and may not have the capacity to

deliver the lncRNA into the subcellular compartment of interest, or to specifically target the cell-type of interest (60), as lncRNAs may have very different functions depending on the cell type (62; 63; 64). Additionally, viral delivery approaches can activate innate and adaptative immune response of the host species, presenting a major limitation to this technology. Overexpression approaches have also been linked with a strong inflammatory response and hepatotoxicity (65). Thus, an exhaustive characterization of lncRNAs is needed for a more efficient targeting. In this study we established that *Chheaf-1* is associated to the chromatin compartment of cardiomyocytes, and that it is enriched in heart tissue, especially in left ventricular cardiomyocytes after pressure overload. These features exalt the potential of *Chheaf-1* as a therapeutic target, as side effects from other cells or organs can be avoided when using gene therapy.

As mentioned before, unlike PCGs, most lncRNAs have low sequence similarity across species, thus, other types of conservation analysis are needed to discover human orthologs. Conservation by synteny has arisen as a logical strategy to identify orthologs, especially for lincRNAs like *Chheaf-1,* whose function is strongly linked to their genomic position. Synteny analysis refers to the succession of genes in the same order and their linear location in the genome of different species (38). However, the presence of a lincRNA in the syntenic region between two species does not always imply orthology. In particular, in presence of a long intergenic region with multiple lincRNAs annotated, the chances of RNA-sequencing artefacts and falsely annotated lincRNA increases (66).To ensure that the *hCHHEAF-1* ortholog is a good candidate, we resort to histone modifications, which play a central role in modulating chromatin structure upon cardiomyocyte hypertrophy. The *Chheaf-1* locus is enriched in H3K27Ac, and regulates H3K27Ac in the promoter region of *Rtn4* in mice. This histone landscape helped us to identify a highly enriched region in the syntenic locus in human, increasing the chance of finding a functional ortholog. Assessing epigenetic marks, including histone modifications to find orthologs is a strategy that has been used by other groups to identify conserved lncRNAs in myogenesis (67). Despite the abovementioned correlations in both mice and human, lincRNA gain- and loss-of-function studies in a human *in vitro* model are required to confirm the effect of *hCHHEAF-1* over *RTN4*.

Thus, using RNA-sequencing, we discovered more than 150 novel lncRNAs dysregulated upon pressure overload. Among them, we characterized *Chheaf-1*, a 600bp lincRNA upregulated upon stress. *Chheaf-1* plays a protective role in the heart and therefore, in the absence of *Chheaf-1*, mice develop severe heart failure after pressure overload. *Chheaf-1*$^{-/-}$ mice have deficient levels of Nogo-A, a protein that mediates sphingolipid synthesis and autophagy. At the onset of hypertrophy, our results suggest an increase of H3K27Ac in the promoter region of *Rtn4*, mediated by *Chheaf-1* bound to Gata4. Blocking the *de novo* sphingolipid synthesis using myriocin, we were able to restore cardiac function and autophagy markers in mice lacking *Chheaf-1*, confirming that the decrease of cardiac function is due to ceramide accumulation and reduced beneficial autophagy. Finally, we identified a human orthologue named *hCHHEAF-1* that follows the same expression pattern of *Chheaf-1* after cardiac stress in patients with failing hearts, thus reinforcing the translational potential of this study.

FUNDING

This project has received funding from the European Union's Horizon 2020 research and innovation programme under the Marie Skłodowska-Curie grant agreement No 813716.

FUTURE PLANS

We have partially characterized the mechanism by which *Chheaf-1* affects H3K27Ac in the promoter of *Rtn4*, however it is not known, whether or not there are third party transcription factors or HDACs/HATs affecting chromatin structure in *Chheaf-1* and *Rtn4 loci*. To discover *Chheaf-1* protein binding partners, we are currently performing ChIRP-MS (comprehensive identification of RNA-binding proteins by mass spectrometry) in samples from TAC cardiomyocytes.

Besides, we are currently studying whether or not *Chheaf-1* binds to chromatin, if so, we intend to map which precise regions of chromatin are *Chheaf-1*-bounded, thus we are performing chromatin Isolation by RNA purification sequencing (ChiRP-Seq). Additionally, we will then confirm if *Chheaf-1* carries out its function acting only in *cis* (thought *Rtn4*) or also in *trans* in cardiomyocytes.

We know that *Chheaf-1* affects H3K27Ac in *Rtn4* promoter though Gata4/p300 at early stages after TAC (1 week) however it is not known yet if this is a prolonged effect, or just occurs immediately after TAC. Thus, we are currently performing ChIP-qPCT experiments mimicking the ones in Fig.4 including further time-points, I.e., 2 and 4 weeks after banding.

To further confirm that the reduced levels in autophagy markers are due to the axis Nogo-A/SPT and sphingolipid dysregulation we are currently performing SPT activity assays in cardiomyocytes of *Chheaf-1*$^{-/-}$ vs. control mice. As Nogo-A is a potent inhibitor of SPT activity. Additionally, to test if the reduced in autophagy alters the mitochondrial ROS production, as it happens in the absence of Nogo-A after banding, we have designed a FACs gating protocol that allows us to evaluate the mitochondrial ROS production in cardiomyocytes using mitoSOX fluorescent dye of mitochondrial ROS species

Further studies are needed to fully characterize *hCHHEAF-1*, for this purpose we are currently deciphering the entire sequence of the transcript by RACE 3' and 5' and norther blotting in samples of human failing hearts. This will allow us to design silencing tools that will be used in *in vitro* human models, to assess whether or not the deletion of *hCHHEAF-1* has an effect over *RTN4*.

BIBLIOGRAPHY

1. Townsend, N., Kazakiewicz, D., Lucy Wright, F., Timmis, A., Huculeci, R., Torbica, A., ... & Vardas, P. (2022). Epidemiology of cardiovascular disease in Europe. Nature Reviews Cardiology, 19(2), 133-143.

2. Abi Khalil, C. (2014). The emerging role of epigenetics in cardiovascular disease. Therapeutic advances in chronic disease, 5(4), 178-187.

3. Movassagh M, Choy MK, Goddard M,Bennett MR, Down TA, Foo RS. Differential DNAmethylation correlates with differential expressionof angiogenic factors in human heart failure. PLoSOne 2010 and 5:e8564.

4. .Haas J, Frese KS, Park YJ, et al. Alterations incardiac DNA methylation in human dilated car-diomyopathy. EMBO Mol Med 2013 and 5:413–29.

5. Meder, B., Haas, J., Sedaghat-Hamedani, F., Kayvanpour, E., Frese, K., Lai, A., ... & Posch, A. E. (2017). Epigenome-wide association study identifies cardiac gene patterning and a novel class of biomarkers for heart failure. Circulation, 136(16), 1528-15.

6. Rauluseviciute, I., Drabløs, F., & Rye, M. B. (2020). DNA hypermethylation associated with upregulated gene expression in prostate cancer demonstrates the diversity of epigenetic regulation. BMC medical genomics, 13(1), 1-15.

7. Zhao Y, Garcia BA. Comprehensive catalogof currently documented histone modifications.Cold Spring Harb Perspect Biol 2015 and 7:a025064.

8. Jenuwein, T., and Allis, C.D. (2001). Translating the histone code. 35–39. Science 293, 1074–1080.

9. Ogryzko, V. V., Schiltz, R. L., Russanova, V., Howard, B. H., & Nakatani, Y. (1996). The transcriptional coactivators p300 and CBP are histone acetyltransferases. Cell, 87(5), 953-959.

10. Takaya, T., Kawamura, T., Morimoto, T., Ono, K., Kita, T., Shimatsu, A., & Hasegawa, K. (2008). Identification of p300-targeted Acetylated Residues in GATA4 during Hypertrophic Responses in Cardiac Myocytes*. Journal of Biological Chemistry, 283(15), 982.

11. Morimoto T, Sunagawa Y, Kawamura T, et al. The dietary compound curcumin inhibits p300 histone acetyltransferase activity and prevents heart failure in rats. J Clin Invest 2008 and 868–78, 118:.

12. Yanazume, T., Hasegawa, K., Morimoto, T., Kawamura, T., Wada, H., Matsumori, A., ... & Kita, T. (2003). Cardiac p300 is involved in myocyte growth with decompensated heart failure. Molecular and cellular biology, 23(10), 3593-3606.

13. Oka, T., Maillet, M., Watt, A. J., Schwartz, R. J., Aronow, B. J., Duncan, S. A., & Molkentin, J. D. (2006). Cardiac-specific deletion of Gata4 reveals its requirement for hypertrophy, compensation, and myocyte viability. Circulation research, 98(6), 837-.

14. Molkentin, J. D., Lu, J. R., Antos, C. L., Markham, B., Richardson, J., Robbins, J., ... & Olson, E. N. (1998). A calcineurin-dependent transcriptional pathway for cardiac hypertrophy. Cell, 93(2), 215-228.

15. Zhou, P., Zhang, Y., Sethi, I., Ye, L., Trembley, M. A., Cao, Y., ... & Pu, W. T. (2022). GATA4 Regulates Developing Endocardium Through Interaction With ETS1. Circulation Research, 131(11), e152-e168.

16. Papait, R., Cattaneo, P., Kunderfranco, P., Greco, C., Carullo, P., Guffanti, A., ... & Condorelli, G. (2013). Genome-wide analysis of histone marks identifying an epigenetic signature of promoters and enhancers underlying cardiac hypertrophy. Proceedings.

17. McKinsey, T. A., Zhang, C. L., & Olson, E. N. (2002). MEF2: a calcium-dependent regulator of cell division, differentiation and death. Trends in biochemical sciences, 27(1), 40-47.

18. Papait, R., Greco, C., Kunderfranco, P., Latronico, M. V., & Condorelli, G. (2013). Epigenetics: a new mechanism of regulation of heart failure?. Basic research in cardiology, 108(4), 1-8.

19. Hang, C. T., Yang, J., Han, P., Cheng, H. L., Shang, C., Ashley, E., ... & Chang, C. P. (2010). Chromatin regulation by Brg1 underlies heart muscle development and disease. Nature, 466(7302), 62-67.

20. Zhang, Y., Huang, Y., Cantalupo, A., Azevedo, P. S., Siragusa, M., Bielawski, J., ... & Di Lorenzo, A. (2016). Endothelial Nogo-B regulates sphingolipid biosynthesis to promote pathological cardiac hypertrophy during chronic pressure overload. JCI insight.

21. Sasset, L., Manzo, O. L., Zhang, Y., Marino, A., Rubinelli, L., Riemma, M. A., ... & Di Lorenzo, A. (2022). Nogo-A reduces ceramide de novo biosynthesis to protect from heart failure. Cardiovascular Research.

22. O'Brien, J., Hayder, H., Zayed, Y., & Peng, C. (2018). Overview of microRNA biogenesis, mechanisms of actions, and circulation. Frontiers in endocrinology, 9, 402.

23. Ikeda, S., He, A., Kong, S. W., Lu, J., Bejar, R., Bodyak, N., ... & Pu, W. T. (2009). MicroRNA-1 negatively regulates expression of the hypertrophy-associated calmodulin and Mef2a genes. Molecular and cellular biology, 29(8), 2193-2204.

24. Huang, Z. P., Chen, J., Seok, H. Y., Zhang, Z., Kataoka, M., Hu, X., & Wang, D. Z. (2013). MicroRNA-22 regulates cardiac hypertrophy and remodeling in response to stress. Circulation research, 112(9), 1234-1243.

25. Yao, R. W., Wang, Y., & Chen, L. L. (2019). Cellular functions of long noncoding RNAs. Nature cell biology, 21(5), 542-551.

26. Wang, K., Long, B. O., Liu, F., Wang, J. X., Liu, C. Y., Zhao, B., ... & Li, P. F. (2016). A circular RNA protects the heart from pathological hypertrophy and heart failure by targeting miR-223. European heart journal, 37(33), 2602-2611.

27. Wang, Y., Zhao, R., Liu, W., Wang, Z., Rong, J., Long, X., ... & Shi, B. (2019). Exosomal circHIPK3 released from hypoxia-pretreated cardiomyocytes regulates oxidative damage in cardiac microvascular endothelial cells via the miR-29a/IGF-1 pathway. Oxidat.

28. Vanamala, J., Reddivari, L., Radhakrishnan, S., & Tarver, C. (2010). Resveratrol suppresses IGF-1 induced human colon cancer cell proliferation and elevates apoptosis via suppression of IGF-1R/Wnt and activation of p53 signaling pathways. BMC cancer, 10(1.

29. Lin, M., Liu, X., Zheng, H., Huang, X., Wu, Y., Huang, A., ... & Huang, Y. (2020). IGF-1 enhances BMSC viability, migration, and anti-apoptosis in myocardial infarction via secreted frizzled-related protein 2 pathway. Stem Cell Research & Therapy, 11(1),.

30. Bär, C., Chatterjee, S., & Thum, T. (2016). Long noncoding RNAs in cardiovascular pathology, diagnosis, and therapy. Circulation, 134(19), 1484-1499.

31. Wang, K., Liu, F., Zhou, L. Y., Long, B., Yuan, S. M., Wang, Y., ... & Li, P. F. (2014). The long noncoding RNA CHRF regulates cardiac hypertrophy by targeting miR-489. Circulation research, 114(9), 1377-1388.

32. Wang, Z., Zhang, X. J., Ji, Y. X., Zhang, P., Deng, K. Q., Gong, J., ... & Wang, Y. (2016). The long noncoding RNA Chaer defines an epigenetic checkpoint in cardiac hypertrophy. Nature medicine, 22(10), 1131-1139.

33. Wang KC, Chang HY. Molecular mechanisms of long noncod- ing RNAs. Mol Cell. 2011 and cel.2011.08.018, 43:904–914. doi: 10.1016/j.mol-.

34. Schoeftner S, Blasco MA. Developmentally regulated transcription of mammalian telomeres by DNA-dependent RNA polymerase II. Nat Cell Biol. 2008 and 10.1038/ncb1685., 10:228–236. doi:.

35. Kowalczyk MS, Hughes JR, Garrick D, Lynch MD, Sharpe JA, Sloane-Stanley JA, McGowan SJ, De Gobbi M, Hosseini M, Vernim- men D, Brown JM, Gray NE, Collavin L, Gibbons RJ, Flint J, Taylor S, Buckle VJ, Milne TA, Wood WG, Higgs DR. Intragenic enhancers act a.

36. Podlevsky JD, Chen JJ. It all comes together at the ends: telomer- ase structure, function, and biogenesis. Mutat Res. 2012 and 10.1016/j.mrfmmm.2011.11.002., 730:3– 11. doi:.

37. Graf, J., & Kretz, M. (2020). From structure to function: Route to understanding lncRNA mechanism. BioEssays, 42(12), 2000027.

38. Camilleri-Robles, C., Amador, R., Klein, C. C., Guigó, R., Corominas, M., & Ruiz-Romero, M. (2022). Genomic and functional conservation of lncRNAs: lessons from flies. Mammalian Genome, 1-15.

39. Louch, W. E., Sheehan, K. A. & Wolska, B. M. Methods in cardiomyocyte isolation, culture, and gene transfer. J Mol Cell Cardiol 51, 288-298, doi:10.1016/j.yjmcc.2011.06.012 (2011).

40. Zhang, D. et al. MTORC1 regulates cardiac function and myocyte survival through 4E-BP1 inhibition in mice. J Clin Invest 120, 2805-2816, doi:10.1172/JCI43008 (2010).

41. Hansmeier, N. R., Widdershooven, P. J., Khani, S., & Kornfeld, J. W. (2019). Rapid generation of long noncoding RNA knockout mice using CRISPR/Cas9 technology. Non-coding RNA, 5(1), 12.

42. deAlmeida, A. C., van Oort, R. J., & Wehrens, X. H. (2010). Transverse aortic constriction in mice. JoVE (Journal of Visualized Experiments), (38), e1729.

43. Peters, A. H. et al. Partitioning and plasticity of repressive histone methylation states in mammalian chromatin. Mol Cell 12, 1577-1589, doi:10.1016/s1097-2765(03)00477-5 (2003).

44. Larcher, V., Kunderfranco, P., Vacchiano, M., Carullo, P., Erreni, M., Salamon, I., ... & Condorelli, G. (2018). An autofluorescence-based method for the isolation of highly purified ventricular cardiomyocytes. Cardiovascular Research, 114(3), 409-416.

45. Taylor, S. C., & Posch, A. (2014). The design of a quantitative western blot experiment. BioMed research international, 2014.

46. Salamon, I., Serio, S., Bianco, S., Pagiatakis, C., Crasto, S., Chiariello, A. M., ... & Condorelli, G. (2020). Divergent transcription of the Nkx2-5 locus generates two enhancer RNAs with opposing functions. IScience, 23(9), 101539.

47. Papait, R., Cattaneo, P., Kunderfranco, P., Greco, C., Carullo, P., Guffanti, A., ... & Condorelli, G. (2013). Genome-wide analysis of histone marks identifying an epigenetic signature of promoters and enhancers underlying cardiac hypertrophy. Proceedings.

48. Gilsbach, R., Schwaderer, M., Preissl, S., Grüning, B. A., Kranzhöfer, D., Schneider, P., ... & Hein, L. (2018). Distinct epigenetic programs regulate cardiac myocyte development and disease in the human heart in vivo. Nature communications, 9(1), 1-14.

49. Liu, X., Ma, Y., Yin, K., Li, W., Chen, W., Zhang, Y., ... & Zhou, Z. (2019). Long non-coding and coding RNA profiling using strand-specific RNA-seq in human hypertrophic cardiomyopathy. Scientific data, 6(1), 1-7.

50. Gilsbach, R., Schwaderer, M., Preissl, S., Grüning, B. A., Kranzhöfer, D., Schneider, P., ... & Hein, L. (2018). Distinct epigenetic programs regulate cardiac myocyte development and disease in the human heart in vivo. Nature communications, 9(1), 1-14.

51. Liu, X., Ma, Y., Yin, K., Li, W., Chen, W., Zhang, Y., ... & Zhou, Z. (2019). Long non-coding and coding RNA profiling using strand-specific RNA-seq in human hypertrophic cardiomyopathy. Scientific data, 6(1), 1-7.

52. Postepska-Igielska, A., Giwojna, A., Gasri-Plotnitsky, L., Schmitt, N., Dold, A., Ginsberg, D., & Grummt, I. (2015). LncRNA Khps1 regulates expression of the proto-oncogene SPHK1 via triplex-mediated changes in chromatin structure. Molecular cell, 60(4),.

53. Xu, Z., Lan, C., Chen, C., Yang, Y., Cao, N., Yu, J., ... & Wu, G. (2022). Heart-enriched long noncoding RNA NPPA-AS1 regulates pathological cardiac hypertrophy by initiating a EP300-GATA4 axis.

54. Xin, M., Davis, C. A., Molkentin, J. D., Lien, C. L., Duncan, S. A., Richardson, J. A., & Olson, E. N. (2006). A threshold of GATA4 and GATA6 expression is required for cardiovascular development. Proceedings of the National Academy of Sciences, 103(30),.

55. Young, M. M., Kester, M., & Wang, H. G. (2013). Sphingolipids: regulators of crosstalk between apoptosis and autophagy. Journal of lipid research, 54(1), 5-19.

56. Nishida, K., Kyoi, S., Yamaguchi, O., Sadoshima, J., & Otsu, K. (2009). The role of autophagy in the heart. Cell Death & Differentiation, 16(1), 31-38.

57. Han, P., Li, W., Lin, C. H., Yang, J., Shang, C., Nurnberg, S. T., ... & Chang, C. P. (2014). A long noncoding RNA protects the heart from pathological hypertrophy. Nature, 514(7520), 102-106.

58. Viereck, J., Kumarswamy, R., Foinquinos, A., Xiao, K., Avramopoulos, P., Kunz, M., ... & Thum, T. (2016). Long noncoding RNA Chast promotes cardiac remodeling. Science translational medicine, 8(326), 326ra22-326ra22.

59. Micheletti, R., Plaisance, I., Abraham, B. J., Sarre, A., Ting, C. C., Alexanian, M., ... & Pedrazzini, T. (2017). The long noncoding RNA Wisper controls cardiac fibrosis and remodeling. Science translational medicine, 9(395), eaai9118.

60. Hobuß, L., Bär, C., & Thum, T. (2019). Long non-coding RNAs: at the heart of cardiac dysfunction?. Frontiers in physiology, 10, 30.

61. Yoshida, T., Morihiro, K., Naito, Y., Mikami, A., Kasahara, Y., Inoue, T., & Obika, S. (2022). Identification of nucleobase chemical modifications that reduce the hepatotoxicity of gapmer antisense oligonucleotides. Nucleic acids research, 50(13), 7224-72.

62. Raveh, E., Matouk, I. J., Gilon, M., & Hochberg, A. (2015). The H19 Long non-coding RNA in cancer initiation, progression and metastasis–a proposed unifying theory. Molecular cancer, 14(1), 1-14.

63. Wang, J., Gibbert, L., Djudjaj, S., Alidousty, C., Rauen, T., Kunter, U., ... & Raffetseder, U. (2016). Therapeutic nuclear shuttling of YB-1 reduces renal damage and fibrosis. Kidney international, 90(6), 1226-1237.

64. Viereck, J., Bührke, A., Foinquinos, A., Chatterjee, S., Kleeberger, J. A., Xiao, K., ... & Thum, T. (2020). Targeting muscle-enriched long non-coding RNA H19 reverses pathological cardiac hypertrophy. European heart journal, 41(36), 3462-3474.

65. Wang, Z., & Zhang, X. (2021). Adenovirus vector-attributed hepatotoxicity blocks clinical application in gene therapy. Cytotherapy, 23(12), 1045-1052.

66. Young, R. S., Marques, A. C., Tibbit, C., Haerty, W., Bassett, A. R., Liu, J. L., & Ponting, C. P. (2012). Identification and properties of 1,119 candidate lincRNA loci in the Drosophila melanogaster genome. Genome biology and evolution, 4(4), 427-442.

67. Bhattacharya, A., Champramary, S., Tripathi, T., Thakur, D., Ioshikhes, I., Singh, S. K., & Nandi, S. (2021). Identification of the conserved long non-coding RNAs in myogenesis. BMC genomics, 22(1), 1-19.

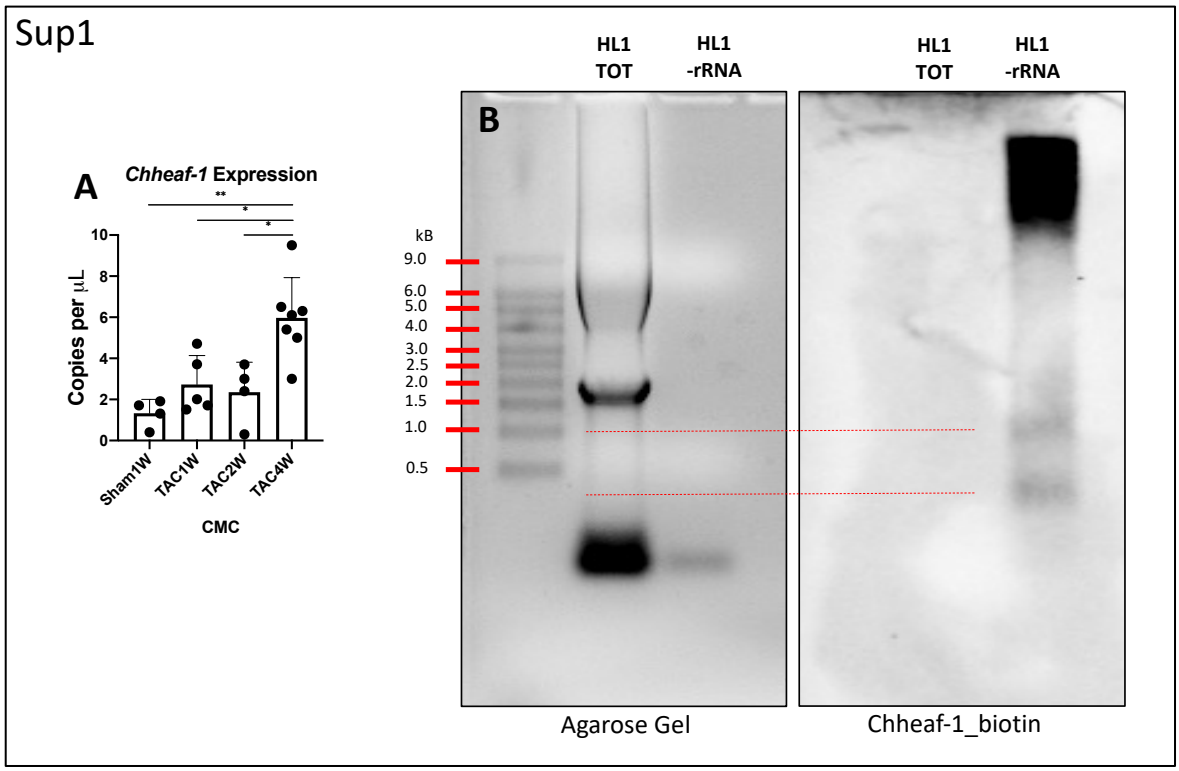

Supplementary Figure 1: *Chheaf*-1 expression pattern and presence in HL-1 cells: (A) *Chheaf-1* expression measured by ddPCR at 1, 2 and 4 weeks after TAC, ordinary one-way Anova with Brown-Forsythe post-hoc was used. p=0.0007 (B) Northern blot using biotin probes for *Chheaf-1* in HL-1 cells with and without rRNA depletion, as indicated.

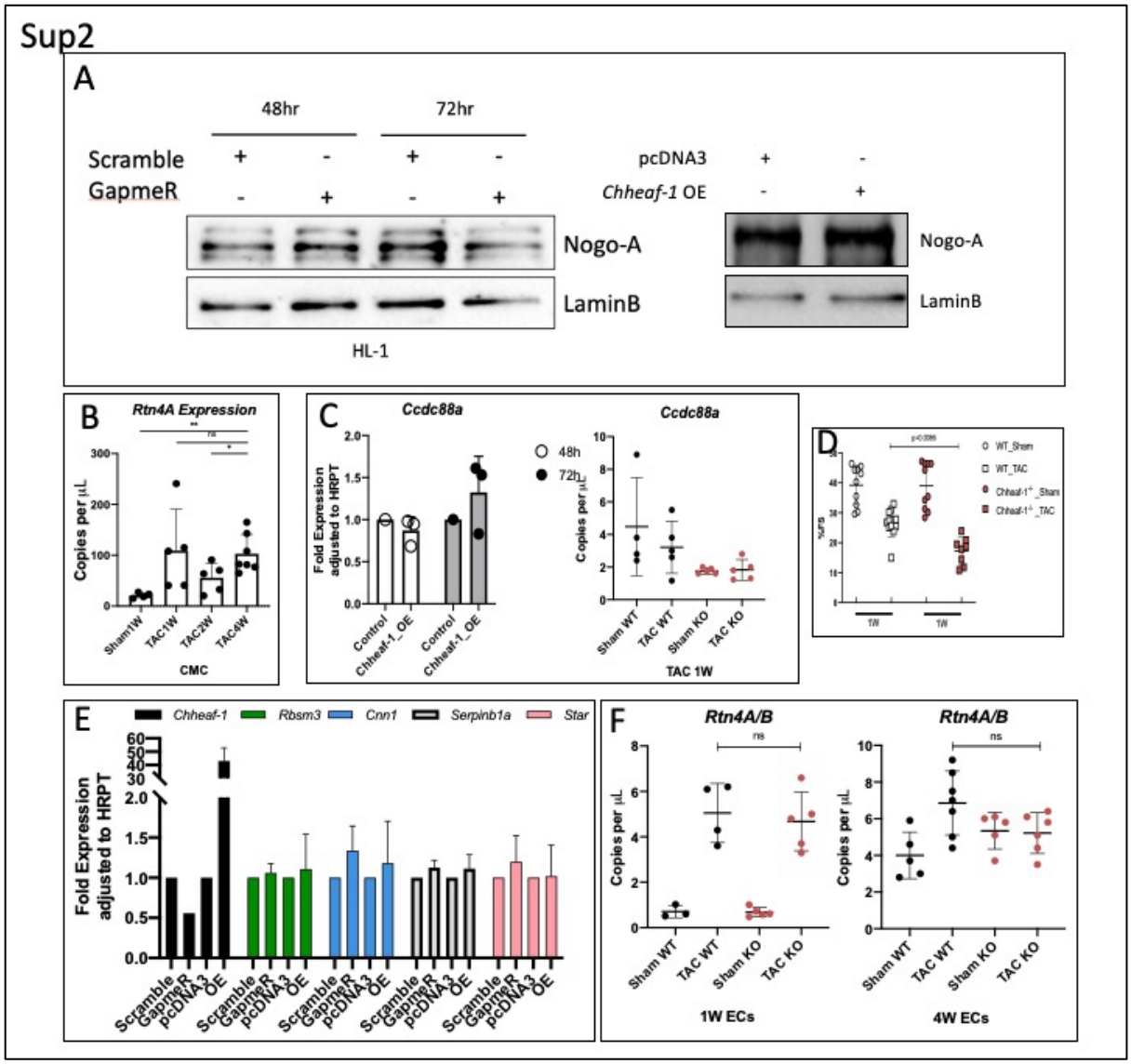

Supplementary Figure 2: *Chheaf-1* regulates Rtn4 expression and protein levels (A)Western blotting in HL1 cells as indicated **Bottom left:** gene expression measured by ddPCR in HL-1 cells transfected with pcDNA3.1-*Chheaf-1* (Transient overexpression with Lipofectamine) **Bottom right**: Western blotting for the same samples (B) ddPCR expression analysis for *Rtn4A* after 1,2 and 4weeks TAC. Ordinary one-way Anova with Brown-Forsythe post-hoc was used. p=0.034 (C) **left**: gene expression of *Ccdc88a* measured by RT-qPCR in HL-1 transfected with pcDNA3.1-*Chheaf-1* (Transient overexpression with Lipofectamine) 48 and 72h after transfection, **right**: *Ccdc88a* expression in CMCs measured with ddPCR after 1 week of TAC (D) Cardiac function assessed by Fractional Shortening 1 week after TAC of control vs Chheaf$^{-/-}$ mice (E) gene expression measured by RT-qPCR in HL-1 cells treated with either GapmeR against *Chheaf-1* or *Chheaf-1* O/E for the 4 genes discovered in the RNA-seq of *Chheaf*$^{-/-}$ vs. control TAC CMC.

Sup 3

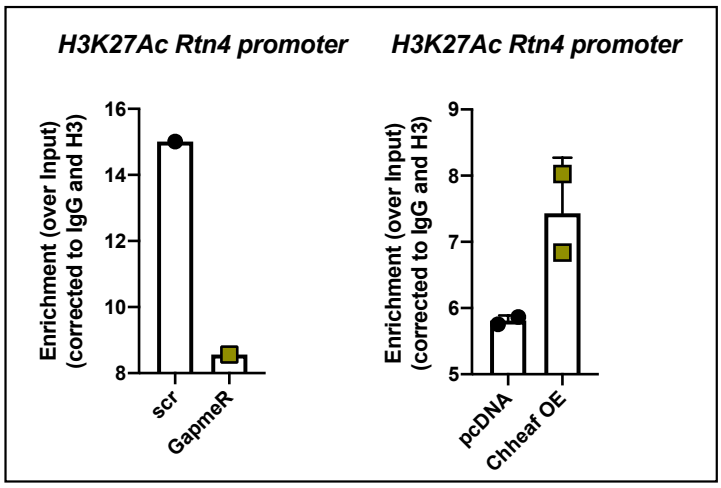

Supplementary Figure 3. *Chheaf-1* regulates H3K27AC in the promoter region of *Rtn4*: **lower part:** ChIP performed in HL-1 cells treated with either GapmeR or *Chheaf-1* overexpression, as indicated, followed by RT-qPCR. Immunoprecipitation was performed with an antibody against H3K27Ac. Graphs show enrichment of H3K27Ac in *Rtn4* and *Chheaf-1 loci*.